

1 **SMN protein is required for normal postnatal development of the spleen**

2

3 Alison K. Thomson<sup>1,3</sup>, Eilidh Somers<sup>2,3</sup>, Rachael A. Powis<sup>2,3</sup>, Hannah K. Shorrock<sup>2,3</sup>,  
4 Kelley Murphy<sup>4</sup>, Kathryn J. Swoboda<sup>5</sup>, Thomas H. Gillingwater<sup>2,3</sup>, Simon H. Parson<sup>1,3</sup>

5

6 <sup>1</sup> University of Aberdeen, Institute of Medical Sciences, Aberdeen, Scotland

7 <sup>2</sup> University of Edinburgh, Centre for Integrative Physiology, Edinburgh, Scotland

8 <sup>3</sup> Euan MacDonald Centre for Motor Neurone Disease Research, Edinburgh, Scotland

9 <sup>4</sup> Department of Biology, Morgan State University, Baltimore, Maryland, USA

10 <sup>5</sup> Massachusetts General Hospital, Department of Neurology, Center for Human  
11 Genetics Research, Boston, MA USA

12

Peer Review Only

1 **Abstract**

2 Spinal Muscular Atrophy (SMA), traditionally described as a predominantly childhood  
3 form of motor neuron disease, is the leading genetic cause of infant mortality.  
4 Although motor neurons are undoubtedly the primary affected cell type, the severe  
5 infantile form of SMA (Type I SMA) is now widely recognised to represent a  
6 multisystem disorder where a variety of organs and systems in the body are also  
7 affected. Here, we report that the spleen is disproportionately small in the  
8 'Taiwanese' murine model of severe SMA (*Smn*<sup>-/-</sup>; *SMN2*<sup>tg/0</sup>), **correlated to low levels**  
9 **of cell proliferation and increased cell death. Spleen** lacks its distinctive red  
10 appearance and presents with a degenerated capsule and a disorganized fibrotic  
11 architecture. Histologically distinct white pulp failed to form and this was reflected in  
12 an almost complete absence of B lymphocytes necessary for normal immune  
13 function. In addition, megakaryocytes persisted in the red pulp. However, the  
14 vascular density remained unchanged in SMA spleen. Assessment of the spleen in  
15 SMA patients with the infantile form of the disease indicated a range of pathologies.  
16 We conclude that development of the spleen fails to occur normally in SMA mouse  
17 models and human patients. Thus, further analysis of immune function is likely to be  
18 required in order to fully understand the full extent of systemic disease pathology in  
19 SMA.  
20

## 1 Introduction

2

3 A significant depletion of the cell-ubiquitous Survival of Motor Neuron (SMN) protein  
4 causes Spinal Muscular Atrophy (SMA). Homozygous deletion or mutation of the  
5 telomeric *SMN1* gene results in a complete failure of functional protein production,  
6 and cell and embryonic survival is only assured by the production of SMN protein by  
7 a centromeric copy gene: *SMN2* (Monani et al., 1999). Due to alternative splicing of  
8 exon 7, *SMN2* produces only ~10% fully functional SMN protein (Monani et al.,  
9 2000). This small amount of SMN protein is sufficient to ensure cell and embryonic  
10 survival, but is insufficient to prevent disease (Monani et al., 1999).

11

12 SMA is the most common inherited cause of infant mortality with a pan-ethnic  
13 incidence of ~1 in 11,000 live births (Sugarman et al., 2012). The disease is primarily  
14 characterised by degeneration of  $\alpha$ -motor neurones in the ventral horn of the spinal  
15 cord, with relative sparing of other cholinergic neuronal populations (Powis and  
16 Gillingwater, 2016). Skeletal muscle atrophy and weakness is generalized in the  
17 infantile phenotype but more severely affects proximal muscles in the intermediate  
18 and milder phenotypes. However, mounting evidence from patients and animal  
19 models suggests that SMA is a multisystem disorder, at least in the most severe  
20 phenotypes with prenatal or early infantile onset of involvement (SMA types 0 and  
21 1; (Hamilton and Gillingwater, 2012, Shababi et al., 2014)). For example, in the more  
22 severe murine models of SMA with juvenile lethality, pathological changes have  
23 been reported in skeletal muscle (Mutsaers et al., 2011), selected brain regions such  
24 as the hippocampus (Wishart et al., 2010), glial cells (Rindt et al., 2015, Hunter et al.,  
25 2014), bone (Shanmugarajan et al., 2009), heart (Shababi et al., 2010), vasculature  
26 (Somers et al., 2012, Somers et al., 2016), lung (Schreml et al., 2012), and pancreas  
27 (Bowerman et al., 2012), with additional recent reports noting defects in testis  
28 (Ottesen et al., 2016) and the gastrointestinal tract (Sintusek et al., 2016). In human  
29 subjects, similar defects have been shown in muscle (Martínez-Hernández et al.,  
30 2009), brain (Ito et al., 2004), heart (Rudnik-Schoneborn et al., 2008), vasculature  
31 (Rudnik-Schoneborn et al., 2010, Araujo et al., 2009, Somers et al., 2016), and  
32 pancreas (Bowerman et al., 2012).

1

2 Preliminary reports have suggested that there may be growth retardation  
3 phenotypes in lymphoid tissues from SMA mice, including thymus and spleen (Dachs  
4 et al., 2011). Given the importance of SMN for vascular development (Somers et al.,  
5 2012, Somers et al., 2016), and the dependence on normal vascularity for  
6 development of the spleen, we were keen to determine the extent to which the  
7 spleen is affected in SMA, as well as the extent to which splenic pathology can be  
8 considered a downstream consequence of defective vascular development and  
9 maturation.

10

11 The spleen fulfils two major functional roles; first, to filter blood by removing  
12 senescent red blood cells in a macrophage filled, sieve-like network of open  
13 sinusoids (Terada et al., 2010); and second, as a secondary lymphoid organ  
14 responsible for the generation of an immune response and innate immunity (Cesta,  
15 2006, Mebius and Kraal, 2005). This immune response arises in the white pulp  
16 compartment of the spleen, where T-cell zones and B-cell follicles initiate antigen-  
17 specific responses necessary to combat blood-borne infections (Bronte and Pittet,  
18 2013). The first crucial stage of white pulp development is the accumulation of B-  
19 cells around the splenic vasculature (Neely and Flajnik, 2015), but as there are no  
20 afferent lymph vessels present in the spleen, influx of leukocytes occurs directly  
21 from the blood (Bronte and Pittet, 2013). Without this aggregation of B-cells no  
22 functional white pulp will form (Myers et al., 2013), while the continued presence of  
23 B-cells supports white pulp maintenance (Wang et al., 2011).

24

25 Here, we report that the spleen appears relatively normal at birth in SMA mice (a  
26 pre-symptomatic time-point), but then fails to match whole animal growth over the  
27 immediate post-natal period as the disease manifests and progresses. It fails to  
28 develop a normal cellular architecture, has significantly decreased cell density and  
29 fails to develop segmented red and white pulp areas. This decreased size and cell  
30 density correlate with **reduced levels of cell proliferation and increased cell death**.  
31 Significantly, there is an almost complete failure of B-cell accumulation, and relative  
32 levels of circulating lymphocytes are decreased. In addition, unusually high

1 concentrations of megakaryocytes are present in the red pulp. Moreover, post-  
2 mortem examination of the spleen in a cohort of SMA type I patients who died from  
3 a variety of causes reveals a range of pathologies, some of which also suggest  
4 abnormal development or acquired splenic dysfunction.

5

For Peer Review Only

## 1 **Materials and Methods**

### 2 **Mice**

3 'Taiwanese' (*Smn*<sup>-/-</sup>;*SMN2*<sup>tg/0</sup>) model of severe SMA and littermate, heterozygous,  
4 control *Smn*<sup>+/-</sup>; *SMN2*<sup>tg/0</sup>: Jackson laboratory stock number 5058) mice were  
5 maintained in the animal care facility at Edinburgh University (Riessland et al., 2010,  
6 Wishart et al., 2014). Mice were retrospectively genotyped using standard PCR  
7 protocols (JAX<sup>®</sup> Mice Resources). The day of birth is designated as P0. All animal  
8 experiments were performed under appropriate personal and project licenses  
9 granted by the UK Home Office, following internal ethical committee approval from  
10 the University of Edinburgh.

11

### 12 **Tissue Collection**

13 Spleens from SMA and control littermates were harvested from mice sacrificed at  
14 P0, P5 and P8 (pre-, mid- and late-symptomatic respectively (Hunter et al., 2016)) by  
15 overdose of anaesthetic (intra-peritoneal injection of pentobarbital) in accordance  
16 with guidelines from the UK Home Office. Spleens were promptly dissected and fixed  
17 in 4% paraformaldehyde (PFA) in 0.1M phosphate buffered saline for 3 hours.  
18 Spleens were weighed post-fixation, and prepared for cryosectioning in 30% sucrose  
19 solution in 0.1M phosphate buffered saline, embedded in OCT at -35°C, sectioned at  
20 8µm and stored at -20°C before staining.

21

### 22 **Quantitative Fluorescent Western Blotting**

23 Spleens were harvested from mice sacrificed at P8 (late-symptomatic) by overdose  
24 of anaesthetic and stored at -80°C. Total protein was isolated and homogenised in  
25 40µl of RIPA buffer (Pierce, Cat No. 89900) with 2.5% proteinase inhibitor cocktail  
26 (Thermo Scientific, Cat No. 1861278). Protein concentrations were determined using  
27 a BCA assay kit (Pierce, Cat No. 23225). Protein was separated by SDS-  
28 polyacrylamide gel electrophoresis on precast NuPage 4-12% Bis-Tris gradient gels  
29 (Thermo Fisher Scientific, Cat No. NP0323) and transferred to a nitrocellulose  
30 membrane using the iBlot<sup>®</sup> 2 Gel Transfer Device (Thermo Fisher Scientific, Cat No.  
31 IB2001) and transfer stack (Thermo Fisher Scientific, Cat No. IB23002). Membranes  
32 were blocked using SEA Block (Thermo Fisher Scientific, Cat No. 37527) and

1 incubated with anti-SMN antibody (BD Biosciences, Cat No. 610646) overnight.  
2 Membranes were incubated for 1.5 hours in donkey anti-mouse IgG H&L AlexaFluor  
3 790 secondary (ab186699). Blots were imaged using an Odyssey Infrared Imaging  
4 System (LI-COR Biosciences). Total protein was measured by incubating a separately  
5 electrophoresed gel in Instant Blue (Expedeon, Cat No. ISB1) for 1 hour and scanning  
6 on the Odyssey Infrared Imaging System. SMN protein levels were normalised to  
7 total protein levels using Image Studio Software (LI-COR Biosciences).

8

### 9 **Histological Staining**

10 Standard haematoxylin and eosin (Cardiff et al., 2014) and picro-sirius red staining  
11 (Junqueira et al., 1979) were performed on sections to observe basic architecture of  
12 the spleen.

13

### 14 **Immunohistochemistry**

15 Sections of spleens were air dried for 30 minutes and blocked in standard blocking  
16 solution (0.4% Bovine Serum Albumin (BSA), 1% Triton X-100 in PBS in 0.1M  
17 phosphate buffered saline) for 45 minutes at room temperature. Sections were then  
18 incubated in primary antibodies overnight at 4°C: PECAM-1 (R&D Systems Cat. No.  
19 AF3628; 1:750); biotinylated CD45R (Life Technologies Cat No. RM2615; 1:200);  
20 CD41 (AbD Serotec Cat. No. MCA2245GA; 1:1000); Ki67 (Abcam Cat. No. ab16667);  
21 and TUNEL in situ cell death kit (Roche Diagnostics Cat No. 11684795910). Sections  
22 were washed and incubated with secondary antibodies for 1 hour at 4°C: Donkey  
23 anti-goat Cy3 (Abcam Cat No. AB6949; 1:250), streptavidin conjugated AlexaFluor  
24 488 (Life Technologies Cat No. S-11223; 1:200), Goat anti-rat AlexaFluor 488 (Abcam  
25 Cat. No. ab150157; 1:200), and Goat anti-rabbit AlexaFluor 568 (Abcam Cat. No.  
26 ab175471). Sections were washed and cover slipped in MOWIOL mounting media  
27 containing DAPI.

28

### 29 **White Blood Cell Differential**

30 P8 control and SMA mice were culled using termination by exsanguination. Under  
31 isoflurane-induced terminal anaesthesia the thoracic cavity was opened and  
32 cardiac puncture to the left ventricle quickly performed. Blood was withdrawn using

1 a 30gauge 0.3ml insulin syringe with one drop of blood used to make a blood smear  
2 (left to air dry) and the remaining placed in a 1.5ml tube with 0.5M EDTA as an  
3 anticoagulant (1:20 ratio with blood) and inverted to mix well. Samples on ice were  
4 immediately taken for WBC differential analysis at the Veterinary Pathology Unit,  
5 University of Edinburgh. Results are expressed as a percentage per 1,000mL of  
6 blood.

7

### 8 **Imaging and Quantification**

9 Microscopy was performed in the Microscope and Histology Core Facility at the  
10 University of Aberdeen. Fluorescent stained slides were viewed using a Zeiss Imager  
11 M2 microscope with Zeiss Apotome, and images were captured with a Zeiss Mrm  
12 digital camera. For nuclear imaging and analysis of cell density a Zeiss confocal  
13 LSM710 microscope and ImageJ were used. Cell Density was calculated using DAPI  
14 labeling and counted using a systematic, random methodology, based on (Mayhew  
15 and Sharma, 1984). Spleens were embedded without specific alignment, and a grid  
16 overlay was placed over a randomly oriented section. From the top left every 3<sup>rd</sup> grid  
17 square was counted (whole nucleus within or touching top and right hand edges  
18 counted, but not counted if touching bottom or left hand edges of sampling box).  
19 Proliferating cells were counted using a modification of this method, separating data  
20 into central and peripheral zones of the spleen. Full grid squares within 100µm of  
21 the edge of the spleen were counted as peripheral; and full grid squares more than  
22 100µm from the edge were counted as central. Data is expressed as cells Per Unit  
23 Area (PUA).

24

25 Quantification of relative vessel area was achieved using ImageJ. PECAM-1 stained  
26 images were converted to binary, and the number of white (PECAM-1 positive) pixels  
27 were counted as a percentage of the total area. This was performed in 10 fields per  
28 spleen from 6 spleens (n=3 for each genotype).

29

### 30 **SMA patient autopsies**

31 Data on type I SMA human subjects was obtained from review of research  
32 documentation obtained at the time of autopsy and from analysis of patient tissues



1 obtained post-mortem. Prior to initiation of any studies, written informed consent  
2 was obtained from the parents to perform a research autopsy under IRB 8751,  
3 reviewed and approved by the University of Utah Institutional Review Board.  
4 Autopsies were performed in collaboration with pathologists at each of the US  
5 institutions involved in this multicenter study (Primary Children's Medical Center and  
6 the Medical Examiner's Office, Salt Lake City, UT; Cook Children's Medical Center, Ft  
7 Worth, TX; Children's Hospital of Atlanta Scottish Rite, Atlanta, GA).

8

### 9 **Statistical Analysis**

10 Analysis and statistical tests were carried out using GraphPad Prism software  
11 (GraphPad Software Inc.). All data are presented as mean  $\pm$  SEM. Unless stated  
12 otherwise, statistical tests were unpaired, two-tailed t-tests, with significance  
13 considered to be  $p < 0.05$ .

14

For Peer Review Only

## 1 Results

2

### 3 The spleen fails to develop correctly in severe SMA mice

4 On initial inspection at birth (P0), there were no gross differences in the form or size  
5 of the spleen between SMA and control littermate mice. However, by P5 dramatic  
6 differences were present, which further increased by P8, when the spleen was very  
7 small and pale in appearance [Fig. 1A]. **We confirmed disease-indicative, low SMN**  
8 **protein levels in SMA spleen by western blot at P8 (Fig 1B).** Quantification confirmed  
9 these qualitative observations, as after birth the spleen failed to increase in size in  
10 SMA mice, and was significantly smaller at both P5 (mid-symptomatic in terms of  
11 neuromuscular pathology: ~87%:  $p < 0.01$ ), and P8 (late symptomatic: ~94%:  
12  $p < 0.0001$ ) compared to control, age-matched littermates [Fig. 1C]. Importantly, the  
13 SMA spleen was disproportionately small, weighing only 0.1% ( $n=3$ ;  $0.1\% \pm 0.002\%$ )  
14 compared to 0.6% ( $n=3$ ;  $0.6\% \pm 0.034$ ) of total body weight in control mice at P8 [Fig  
15 1D].

16

17 To further investigate the basis of this postnatal developmental phenotype, cell  
18 density was measured by counting DAPI-stained cell nuclei. Cell density increased in  
19 control spleens from birth to P5 and then was maintained at a relatively consistent  
20 level until P8 (P0  $9.96 \pm 1.03$  PUA,  $n=3$ ; P5  $18.03 \pm 0.82$  PUA,  $n=3$ ). SMA spleen showed  
21 a similar pattern until P5, with no significant differences from control (P0  $11.0 \pm 1.77$   
22 PUA,  $n=3$ ; P5  $15.8 \pm 2.57$  PUA,  $n=3$ ), but by P8 cell density in the spleen was  
23 significantly reduced (<50%) ( $6.83 \pm 0.91$  cells per unit area: PUA,  $n=3$ ; P8  $p < 0.005$ )  
24 compared with control littermates ( $15.58 \pm 1.22$  PUA;  $n=3$ ; P8) [Fig. 1E].

25 In summary, the spleen appeared normal at birth in SMA mice, but then failed to  
26 grow and develop correctly, lacking the internal organisation observed in the spleen  
27 from healthy control animals.

28

### 29 **Altered proliferation and cell death profiles underlie decreased spleen size**

30 **Given the significant difference in size and cell density between control and SMA**  
31 **spleens, we sought to further investigate this by analysing the distribution of**  
32 **proliferating and apoptotic cells. In the pre-symptomatic spleen (P0), numbers of**

1 proliferating cells in both control and SMA spleens were relatively high, and evenly  
2 distributed throughout the spleen [Fig. 2A]. By the mid-symptomatic stage (P5) there  
3 were significantly greater numbers of proliferating cells in the periphery of the SMA  
4 spleen ( $18.67 \pm 0.5$  PUA;  $n=3$ ; P5  $p < 0.001$ ) compared with the periphery of control  
5 spleen ( $15.0 \pm 0.71$  PUA,  $n=3$ ; P5) [Fig. 2B]. Conversely, at this point proliferation in  
6 the centre was dramatically reduced in control and SMA spleens (Control:  $3.0 \pm 0.69$ ,  
7  $n=3$ ; SMA;  $3.67 \pm 1.04$ ,  $n=3$ ; P5). Interestingly, at P8 there was a significant decrease in  
8 proliferating cell numbers in both the centre and periphery of the SMA spleen [Fig.  
9 2C] (centre:  $p < 0.0001$ ;  $0.88 \pm 0.35$ ,  $n=3$ ; P8; periphery:  $p < 0.005$ ;  $5.88 \pm 0.53$ ,  $n=3$ ; P8),  
10 compared with the control spleen (centre:  $8.44 \pm 0.92$ ,  $n=3$ ; P8; periphery;  $9.0 \pm 0.74$ ,  
11  $n=3$ ; P8). The general pattern suggests that proliferation falls dramatically in the late  
12 symptomatic SMA spleen.

13 On initial observation of the pre-symptomatic spleen (P0), cell death was more  
14 prevalent at the periphery of the spleen in both control and SMA mice, however  
15 there was no significant difference between the two [Fig. 2D]. By the mid-  
16 symptomatic (P5) stage there were  $\sim 7x$  more apoptotic cells at the periphery of the  
17 SMA spleen [Fig. 2E] ( $****p < 0.0001$ ;  $2.62 \pm 0.31$  PUA,  $n=3$ ; P5) compared with the  
18 control spleen ( $0.36 \pm 0.27$  PUA,  $n=3$ ). The apoptotic cells appeared to be confined to  
19 the extreme periphery and were likely capsule cells. Finally, by late-symptomatic  
20 stage (P8) cell death occurred more uniformly throughout the splenic tissue in both  
21 control and SMA spleens [Fig. 2F], with no significant differences. In summary, cell  
22 death was generally variable but relatively low throughout all regions, and between  
23 SMA and control spleens. The exception was at P5 where there was a dramatic  
24 increase in cell death in peripheral cells in SMA spleen.

25  
26 **Morphologically distinct white pulps fails to develop and ultimately the spleen**  
27 **begins to degenerate in SMA mice**

28 Next, we used haematoxylin and eosin stained histological preparations from SMA  
29 and control mouse spleen to assess cellular morphology. At P0 the white pulp had  
30 not aggregated in control spleen and there were no clear differences between  
31 control and SMA spleen (data not shown). In control spleen at P8, as expected,  
32 clearly differentiated islands of white pulp surrounding central arterioles within a

1 mass of red pulp were present, and the surrounding capsule and centrally projecting  
2 fingers of trabeculae were well developed [Fig 3A]. However, in SMA spleen the  
3 appearance was strikingly different. Here, the tissue appeared homogeneous, with  
4 no apparent segregation of white pulp, and an overall appearance most closely  
5 resembling homogeneous red pulp [Fig.3D]. This suggests either a failure to develop,  
6 or incomplete migration and segregation of cells into red and white pulp areas. In  
7 addition, no clear capsule was observed surrounding the SMA spleen [Fig. 3E], which  
8 may account for its very fragile nature at dissection. To further examine this, we  
9 used Picro Sirius Red to stain the collagen fibres, which are a major constituent of  
10 the capsule and trabeculae. Control spleen had a well developed and organised  
11 fibrous framework, as predicted [Fig. 3C], while SMA spleen showed almost no  
12 collagen where the capsule should be present and a highly disorganised internal  
13 arrangement [Fig. 3F]. This indicates the presence of fibrosis and degenerative  
14 processes within the spleen of SMA mice.

15

#### 16 **Vascular density is not affected in the SMA spleen**

17 To further understand the aetiology of the aberrant lymphoid tissue development in  
18 SMA spleen, we turned our attention to its vascular supply. As a blood filter, the  
19 vascular development within the spleen is critical for proper function (Cesta, 2006).  
20 We carried out PECAM-1 (an endothelial cell marker) immunohistochemistry on  
21 spleens from P0, P5 and P8 mice. Initial qualitative observations showed no apparent  
22 difference in either the form or density of the vascular component in SMA mice [Fig  
23 4]. Quantitative assessment of the vasculature at each time point confirmed that  
24 there were no differences between SMA and control spleens (SMA P0,  $4.94\% \pm 0.66$ ;  
25 control P0,  $6.39\% \pm 0.57$ ; SMA P5,  $5.21\% \pm 0.29$ ; control P5,  $4.63\% \pm 0.77$ ; SMA P8,  
26  $5.92\% \pm 0.42$ ; control P8,  $6.38\% \pm 0.29$ ) [Fig 4]. Thus, the defects observed in the spleen  
27 of SMA mice are unlikely to represent a secondary consequence of vascular defects  
28 previously reported elsewhere in the body (Somers et al., 2012, Somers et al., 2016).

29

#### 30 **Developing B-cell follicles are absent in SMA spleen**

31 To further investigate the apparent failure of white pulp aggregation in SMA spleen,  
32 we next examined B-cell lymphocytes, which are necessary for normal immune

1 functions of the spleen. CD45R (a pan B-cell marker) in conjunction with PECAM-1  
2 (as above) immunohistochemistry showed regular accumulations of brightly stained  
3 B-cells in control animals, indicative of developing white pulp from P5 onwards [Fig.  
4 5]. Significantly, these were not present in SMA spleen, where only diffuse,  
5 homogeneously distributed and poorly stained B-cells were present. We next carried  
6 out a white blood cell differential blood analysis. This revealed a significantly lower  
7 percentage (\*\* $p < 0.01$ ) of circulating lymphocytes in the SMA mouse ( $31.7\% \pm 2.77$ ,  
8  $n=4$ ) compared with control mice ( $55.25\% \pm 3.96$ ,  $n=4$ ) [Fig. 5]. Taken together these  
9 findings reveal a striking absence of resident lymphocytes (B-cell follicles) in the  
10 spleen and a similar reduction in circulating lymphocytes in SMA mice.

11

### 12 **Megakaryocyte populations are increased in SMA spleen**

13 Further examination of haematoxylin and eosin stained histological preparations  
14 from SMA and control mouse spleen revealed the presence of many large cells with  
15 lobulated nuclei [Fig. 3G], which we suspected to be megakaryocytes, in SMA  
16 samples. We sought to confirm this by performing immunohistochemical staining  
17 with antibodies against CD41 (a megakaryocyte cell and platelet marker) in control  
18 and late-symptomatic mice [Fig 6. A, B]. We identified megakaryocytes by co-staining  
19 with a DAPI nuclear stain [Fig 6. A, B. inset], as platelets do not contain nuclei.  
20 Quantitative analysis revealed significantly greater numbers (\*\*\*\* $p < 0.0001$ ) of  
21 megakaryocytes in late symptomatic P8 SMA spleen ( $5.9 \pm 0.56$ ,  $n=3$ : mean  $\pm$  SEM;  
22 p8) compared to control spleens ( $1.13 \pm 0.18$  PUA,  $n=3$ ; p8) [Fig 6C].

23

### 24 **Preliminary observations of spleen abnormalities in SMA type I patients**

25 We were keen to establish whether any of the defects found in mouse models were  
26 similarly present in human SMA patients. Autopsy samples collected from severe  
27 SMA patients ( $n=9$ , SMA type I) aged 6-60 months, revealed that 56% (5 of 9) of  
28 patients demonstrated abnormal splenic pathology, either grossly or upon further  
29 examination of tissues via light microscopy (Table 1). Observed changes included  
30 gross defects such as increased white pulp, small accessory spleens, and congestion  
31 and presence of erythroid precursors in the red pulp. These findings confirm that  
32 abnormalities in the spleen occur in at least a subset of patients with SMA type I.

1

For Peer Review Only

## 1 Discussion

2 Given the historical context of SMA as a clinically-defined motor neuron disease,  
3 most previous research has understandably focussed on key pathological events  
4 surrounding motor neuron loss and muscle atrophy. However, as the protein  
5 product of the *SMN* gene is expressed ubiquitously in all cells and tissues of the  
6 body, we should perhaps not be surprised that depletion of *SMN* in SMA results in  
7 pathologies affecting other organ and tissue systems (Hamilton and Gillingwater,  
8 2012, Shababi et al., 2014). Here, we extend these findings to reveal significant  
9 defects in the gross anatomy and cellular composition of the spleen in an established  
10 mouse model of severe SMA. The spleen was disproportionately small and had a  
11 disturbed architecture, most notable changes were failed B-cell aggregation in white  
12 pulp and an abnormal amount of megakaryocytes present in red pulp. In contrast,  
13 the basic vasculature of the spleen appeared to be unaffected. The defects described  
14 here reflect failed post-natal development of the spleen, resulting in a grossly  
15 deficient and defective organ at postnatal day 10, when these mice display severe  
16 neuromuscular pathology. Importantly, a range of pathologies were also seen at  
17 autopsy in severe SMA patients.

18

19 We have previously reported significant depletion of capillary beds in skeletal muscle  
20 and spinal cord of SMA mice and human SMA patients (Somers et al., 2011, Somers  
21 et al., 2016), resulting in functionally-significant tissue hypoxia (Somers et al., 2016).

22 We expected to find a similar pathology in the spleen of SMA mice, but were  
23 surprised to find that although the spleen was small and pale in appearance, the  
24 density of the intrinsic vasculature remained unchanged. However, it should be  
25 noted that the vascular development of the spleen is significantly different to that in  
26 muscle and spinal cord. In most organs, vessel ingrowth determines organ growth,  
27 while in muscle and central nervous system, the vasculature grows into expanding  
28 organ systems (Ramasamy et al., 2015, Crivellato et al., 2007). As the SMA spleen is  
29 approximately 20 times smaller, in absolute terms, than the control spleen at late  
30 stages, this could reflect decreased angiogenesis, which then fails to drive organ  
31 expansion. **Equally, low numbers of lymphocytes are present in the spleen at birth,**  
32 **while high levels of proliferating B and T-cells are present in order to form a**

1 functioning white pulp capable of providing immune responses (Loder et al., 1999,  
2 Le Campion et al., 2002). Therefore, it is unsurprising that the late-symptomatic SMA  
3 spleen with no white pulp has significantly fewer proliferating cells, especially  
4 centrally, where white pulp should be developing. The increased levels of cell  
5 proliferation in the periphery of the SMA spleen at P5 suggest an attempt to  
6 maintain normal splenic growth, however this is countered by a simultaneous  
7 increase in cell death at the periphery. Interestingly, cell death appears to occur  
8 largely in the splenic capsule of the mid-symptomatic SMA spleen, an area we have  
9 shown to be fibrotic and degenerative. The subsequent decrease in cell proliferation  
10 both centrally and peripherally at P8 in the SMA spleen correlates with our reports  
11 of small spleen size and decreased cell density.

12 The decrease in circulating lymphocytes coupled with the failure of B-cells to  
13 accumulate and form a functional white pulp in SMA mice, suggests a developmental  
14 defect in the immune system. B-cells are generated in bone marrow and must travel  
15 via the circulatory system to the spleen and through the T-cell zone, where they  
16 communicate with activated T-cells and subsequently mature (Forster et al., 1999,  
17 Mebius and Kraal, 2005). Vascular endothelial cells in the spleen are critical for this  
18 lymphocyte homing behaviour from high endothelial venules (Czompoly et al., 2011,  
19 Lee et al., 2014), and a subtle defect in the endothelial cells could lie at the root of  
20 this. However, the decrease in numbers of circulating lymphocytes in the blood  
21 suggests that B-cells may simply not be present in sufficient numbers to aggregate in  
22 the spleen. The spleen should normally contain approximately 25% of the total  
23 number of lymphocytes (Nolte et al., 2002) and the absence of B-cell lymphocytes in  
24 the SMA spleen may be an indicator of a more widespread defect in the immune  
25 system.

26

27 In the red pulp, we observed an increase in the number of megakaryocytes in SMA  
28 spleen. This evidence of extra-medullary haematopoiesis is suggestive of a secondary  
29 response to a systemic change, most likely hypoxia (Kim, 2010), and we have  
30 previously reported significant hypoxia in these mice at P5 (Somers et al., 2016).  
31 Extra-medullary haematopoiesis, as suggested by the increase in red pulp  
32 megakaryocytes, has been linked to a loss of splenic architecture (Franke et al.,



1 2013) and may be responsible for the generally disorganised splenic microstructure  
2 in SMA.

3 We were interested to determine if any changes in gross morphology were present  
4 in the spleen of severe SMA patients, which the mice used in this study most closely  
5 model (Hsieh-Li et al., 2000). When data from routine autopsies were reviewed, we  
6 found that the majority showed some gross or micro-anatomical pathology. The fact  
7 that these abnormalities include both what could be termed developmental and  
8 degenerative pathologies, suggests that the human spleen is a focus of previously  
9 un-described pathology in severe patients and warrants further investigation.

10 **Given that the majority of the defects we have observed in the mouse model would**  
11 **not be observable at routine autopsy, it is perhaps not surprising that several patient**  
12 **spleens appear 'normal' in macroscopic appearance. However, the variability of both**  
13 **patient age and observed splenic abnormalities, including absence in some cases,**  
14 **suggests that further studies are required to examine potential parallels with**  
15 **observations from the SMA mouse model.**

16 In summary, we show that SMN depletion leads to specific yet varied defects in the  
17 gross and microanatomy of the spleen in a mouse model of severe SMA. Further, a  
18 range of splenic defects were present in severe SMA patients. This is likely to lead to  
19 a significantly compromised immune system in SMA that may have important  
20 implications for the broader spectrum of pathology that occurs in the disease.

21

## 22 **Acknowledgements**

23 The authors would like to acknowledge the Microscopy and Histology Core Facility at  
24 the University of Aberdeen for the use of their facilities; members of the Gillingwater  
25 lab at Edinburgh University for tissue collection and guidance; and the Anatomical  
26 Society for funding this research. We are forever grateful to the patients and families  
27 who supported these efforts by participating in research studies.

28

## 29 **Funding**

30 SHP received an Anatomical Society PhD Studentship award for AKT

- 1 THG received an Anatomical Society PhD Studentship award for RAP and funding
- 2 from the SMA Trust (UK SMA Research Consortium), Euan MacDonald Centre for
- 3 Motor Neurone Disease Research, and Muscular Dystrophy UK.
- 4 KJS received funding for pathologic studies in human subjects from NICHD grant R01-
- 5 HD054599.
- 6

For Peer Review Only

1 **References**

- 2 Araujo A, Araujo M, Swoboda KJ (2009) Vascular perfusion abnormalities in  
3 infants with spinal muscular atrophy. *J Pediatr*, **155**, 292-4.
- 4 Bowerman M, Swoboda KJ, Michalski JP, et al. (2012) Glucose metabolism and  
5 pancreatic defects in spinal muscular atrophy. *Ann Neurol*, **72**, 256-68.
- 6 Bronte V, Pittet MJ (2013) The spleen in local and systemic regulation of  
7 immunity. *Immunity*, **39**, 806-18.
- 8 Cardiff RD, Miller CH, Munn RJ (2014) Manual hematoxylin and eosin staining of  
9 mouse tissue sections. *Cold Spring Harb Protoc*, **2014**, 655-8.
- 10 Cesta MF (2006) Normal structure, function, and histology of the spleen.  
11 *Toxicologic pathology*, **34**, 455-465.
- 12 Crivellato E, Nico B, Ribatti D (2007) Contribution of endothelial cells to  
13 organogenesis: a modern reappraisal of an old Aristotelian concept. *J*  
14 *Anat*, **211**, 415-27.
- 15 Czompoly T, Labadi A, Kellermayer Z, Olasz K, Arnold HH, Balogh P (2011)  
16 Transcription factor Nkx2-3 controls the vascular identity and  
17 lymphocyte homing in the spleen. *J Immunol*, **186**, 6981-9.
- 18 Dachs E, Hereu M, Piedrafita L, Casanovas A, Calderó J, Esquerda JE (2011)  
19 Defective neuromuscular junction organization and postnatal myogenesis  
20 in mice with severe spinal muscular atrophy. *Journal of Neuropathology &*  
21 *Experimental Neurology*, **70**, 444-461.
- 22 Forster R, Schubel A, Breitfeld D, et al. (1999) CCR7 coordinates the primary  
23 immune response by establishing functional microenvironments in  
24 secondary lymphoid organs. *Cell*, **99**, 23-33.
- 25 Franke K, Kalucka J, Mamlouk S, et al. (2013) HIF-1alpha is a protective factor in  
26 conditional PHD2-deficient mice suffering from severe HIF-2alpha-  
27 induced excessive erythropoiesis. *Blood*, **121**, 1436-45.
- 28 Hamilton G, Gillingwater TH (2012) Spinal muscular atrophy: going beyond the  
29 motor neuron. *Trends in molecular medicine*.
- 30 Hsieh-Li HM, Chang JG, Jong YJ, et al. (2000) A mouse model for spinal muscular  
31 atrophy. *Nat Genet*, **24**, 66-70.
- 32 Hunter G, Aghamaleky Sarvestany A, Roche SL, Symes RC, Gillingwater TH  
33 (2014) SMN-dependent intrinsic defects in Schwann cells in mouse  
34 models of spinal muscular atrophy. *Hum Mol Genet*, **23**, 2235-50.
- 35 Hunter G, Powis RA, Jones RA, et al. (2016) Restoration of SMN in Schwann cells  
36 reverses myelination defects and improves neuromuscular function in  
37 spinal muscular atrophy. *Hum Mol Genet*.
- 38 Ito Y, Kumada S, Uchiyama A, et al. (2004) Thalamic lesions in a long-surviving  
39 child with spinal muscular atrophy type I: MRI and EEG findings. *Brain*  
40 *Dev*, **26**, 53-6.
- 41 Junqueira LC, Bignolas G, Brentani RR (1979) Picrosirius staining plus  
42 polarization microscopy, a specific method for collagen detection in tissue  
43 sections. *Histochem J*, **11**, 447-55.
- 44 Kim CH (2010) Homeostatic and pathogenic extramedullary hematopoiesis. *J*  
45 *Blood Med*, **1**, 13-9.
- 46 Le Campion A, Bourgeois C, Lambolez F, et al. (2002) Naive T cells proliferate  
47 strongly in neonatal mice in response to self-peptide/self-MHC  
48 complexes. *Proc Natl Acad Sci U S A*, **99**, 4538-43.

- 1 Lee M, Kiefel H, LaJevic MD, et al. (2014) Transcriptional programs of lymphoid  
2 tissue capillary and high endothelium reveal control mechanisms for  
3 lymphocyte homing. *Nat Immunol*, **15**, 982-95.
- 4 Loder F, Mutschler B, Ray RJ, et al. (1999) B cell development in the spleen takes  
5 place in discrete steps and is determined by the quality of B cell receptor-  
6 derived signals. *J Exp Med*, **190**, 75-89.
- 7 Martínez-Hernández R, Soler-Botija C, Also E, et al. (2009) The developmental  
8 pattern of myotubes in spinal muscular atrophy indicates prenatal delay  
9 of muscle maturation. *Journal of Neuropathology & Experimental*  
10 *Neurology*, **68**, 474-481.
- 11 Mayhew TM, Sharma AK (1984) Sampling schemes for estimating nerve fibre  
12 size. I. Methods for nerve trunks of mixed fascicularity. *J Anat*, **139 ( Pt 1)**,  
13 45-58.
- 14 Mebius RE, Kraal G (2005) Structure and function of the spleen. *Nat Rev*  
15 *Immunol*, **5**, 606-16.
- 16 Monani UR, Lorson CL, Parsons DW, et al. (1999) A single nucleotide difference  
17 that alters splicing patterns distinguishes the SMA gene SMN1 from the  
18 copy gene SMN2. *Hum Mol Genet*, **8**, 1177-83.
- 19 Monani UR, Sendtner M, Coover DD, et al. (2000) The human centromeric  
20 survival motor neuron gene (SMN2) rescues embryonic lethality in Smn-  
21 /- mice and results in a mouse with spinal muscular atrophy. *Human*  
22 *Molecular Genetics*, **9**, 333-339.
- 23 Mutsaers CA, Wishart TM, Lamont DJ, et al. (2011) Reversible molecular  
24 pathology of skeletal muscle in spinal muscular atrophy. *Hum Mol Genet*,  
25 **20**, 4334-44.
- 26 Myers RC, King RG, Carter RH, Justement LB (2013) Lymphotoxin alpha1beta2  
27 expression on B cells is required for follicular dendritic cell activation  
28 during the germinal center response. *Eur J Immunol*, **43**, 348-59.
- 29 Neely HR, Flajnik MF (2015) CXCL13 responsiveness but not CXCR5 expression  
30 by late transitional B cells initiates splenic white pulp formation. *J*  
31 *Immunol*, **194**, 2616-23.
- 32 Nolte MA, Hamann A, Kraal G, Mebius RE (2002) The strict regulation of  
33 lymphocyte migration to splenic white pulp does not involve common  
34 homing receptors. *Immunology*, **106**, 299-307.
- 35 Ottesen EW, Howell MD, Singh NN, Seo J, Whitley EM, Singh RN (2016) Severe  
36 impairment of male reproductive organ development in a low SMN  
37 expressing mouse model of spinal muscular atrophy. *Sci Rep*, **6**, 20193.
- 38 Powis RA, Gillingwater TH (2016) Selective loss of alpha motor neurons with  
39 sparing of gamma motor neurons and spinal cord cholinergic neurons in a  
40 mouse model of spinal muscular atrophy. *J Anat*, **228**, 443-51.
- 41 Ramasamy SK, Kusumbe AP, Adams RH (2015) Regulation of tissue  
42 morphogenesis by endothelial cell-derived signals. *Trends Cell Biol*, **25**,  
43 148-57.
- 44 Riessland M, Ackermann B, Forster A, et al. (2010) SAHA ameliorates the SMA  
45 phenotype in two mouse models for spinal muscular atrophy. *Hum Mol*  
46 *Genet*, **19**, 1492-506.
- 47 Rindt H, Feng Z, Mazzasette C, et al. (2015) Astrocytes influence the severity of  
48 spinal muscular atrophy. *Hum Mol Genet*, **24**, 4094-102.

- 1 Rudnik-Schoneborn S, Heller R, Berg C, et al. (2008) Congenital heart disease is a  
2 feature of severe infantile spinal muscular atrophy. *J Med Genet*, **45**, 635-  
3 8.
- 4 Rudnik-Schoneborn S, Vogelgesang S, Armbrust S, Graul-Neumann L, Fusch C,  
5 Zerres K (2010) Digital necroses and vascular thrombosis in severe spinal  
6 muscular atrophy. *Muscle Nerve*, **42**, 144-7.
- 7 Schreml J, Riessland M, Paterno M, et al. (2012) Severe SMA mice show organ  
8 impairment that cannot be rescued by therapy with the HDACi JNJ-  
9 26481585. *European Journal of Human Genetics*.
- 10 Shababi M, Habibi J, Yang HT, Vale SM, Sewell WA, Lorson CL (2010) Cardiac  
11 defects contribute to the pathology of spinal muscular atrophy models.  
12 *Hum Mol Genet*, **19**, 4059-71.
- 13 Shababi M, Lorson CL, Rudnik-Schoneborn SS (2014) Spinal muscular atrophy: a  
14 motor neuron disorder or a multi-organ disease? *J Anat*, **224**, 15-28.
- 15 Shanmugarajan S, Tsuruga E, Swoboda KJ, Maria BL, Ries WL, Reddy SV (2009)  
16 Bone loss in survival motor neuron (Smn<sup>-/-</sup> SMN2) genetic mouse model  
17 of spinal muscular atrophy. *The Journal of pathology*, **219**, 52-60.
- 18 Sintusek P, Catapano F, Angkathunkayul N, et al. (2016) Histopathological  
19 Defects in Intestine in Severe Spinal Muscular Atrophy Mice Are Improved  
20 by Systemic Antisense Oligonucleotide Treatment. *PLoS One*, **11**,  
21 e0155032.
- 22 Somers E, Lees RD, Hoban K, et al. (2016) Vascular Defects and Spinal Cord  
23 Hypoxia in Spinal Muscular Atrophy. *Ann Neurol*, **79**, 217-30.
- 24 Somers E, Stencel Z, Wishart TM, Gillingwater TH, Parson SH (2011) Density,  
25 calibre and ramification of muscle capillaries are altered in a mouse  
26 model of severe spinal muscular atrophy. *Neuromuscular Disorders*.
- 27 Somers E, Stencel Z, Wishart TM, Gillingwater TH, Parson SH (2012) Density,  
28 calibre and ramification of muscle capillaries are altered in a mouse  
29 model of severe spinal muscular atrophy. *Neuromuscul Disord*, **22**, 435-  
30 42.
- 31 Sugarman EA, Nagan N, Zhu H, et al. (2012) Pan-ethnic carrier screening and  
32 prenatal diagnosis for spinal muscular atrophy: clinical laboratory  
33 analysis of >72,400 specimens. *Eur J Hum Genet*, **20**, 27-32.
- 34 Terada N, Saitoh Y, Saitoh S, Ohno N, Jin T, Ohno S (2010) Visualization of  
35 microvascular blood flow in mouse kidney and spleen by quantum dot  
36 injection with "in vivo cryotechnique". *Microvasc Res*, **80**, 491-8.
- 37 Wang X, Cho B, Suzuki K, et al. (2011) Follicular dendritic cells help establish  
38 follicle identity and promote B cell retention in germinal centers. *J Exp*  
39 *Med*, **208**, 2497-510.
- 40 Wishart TM, Huang JP-W, Murray LM, et al. (2010) SMN deficiency disrupts brain  
41 development in a mouse model of severe spinal muscular atrophy. *Human*  
42 *molecular genetics*, **19**, 4216-4228.
- 43 Wishart TM, Mutsaers CA, Riessland M, et al. (2014) Dysregulation of ubiquitin  
44 homeostasis and beta-catenin signaling promote spinal muscular atrophy.  
45 *J Clin Invest*, **124**, 1821-34.
- 46  
47

1 **Figure Legends**

2

3 **Figure 1. SMA spleen is disproportionately small and disorganised**

4 **A.** Spleen from control (left) and late symptomatic (P8) SMA (right) mice. SMA spleen

5 appears dramatically smaller and pale in comparison to control spleen. Scale bar =

6 5mm. **B.** Quantitative western blot of SMN protein (green) displays a significant

7 reduction of SMN (~40kDa) in late-symptomatic (P8) SMA spleens ( $p < 0.0001$ ; ~39%)

8 compared with controls. **C.** Spleen weights at pre- (P0), mid- (P5), and late-

9 symptomatic (P8) time points. SMA spleens are significantly smaller than control

10 spleens at both P5 (\*\* $p < 0.005$ ) and P8 (\*\*\*\* $p < 0.0001$ ).

11 **D.** As a percentage of total body weight, spleens are significantly smaller at both p5 (\*\*  $p < 0.05$ ) and P8

12 (\*\*\*\* $p < 0.0001$ ). **E.** Quantification shows a significantly reduced density of cells in the

13 SMA spleen (\*\* $p < 0.01$ ).

14

1 **Figure 2. Cell proliferation and cell death are altered in the SMA spleen**  
2 Cell proliferation marker Ki67 (red) and cell death marker TUNEL (green) staining of  
3 pre-, mid- and late-symptomatic mice. **A.** At the pre-symptomatic stage (P0) cell  
4 proliferation is occurring uniformly throughout splenic tissue in both control and  
5 SMA mice. **B.** At the mid-symptomatic stage (P5) there is a significant increase in cell  
6 proliferation in the periphery of the SMA spleen (\*\* $p < 0.005$ ). **C.** At the late-  
7 symptomatic stage (P8) cell proliferation is significantly reduced both centrally  
8 (\*\* $p < 0.0001$ ) and peripherally (\*\* $p < 0.01$ ) in SMA mice. Scale bar = 100 $\mu$ m. **D.** At  
9 birth (P0), apoptosis is largely restricted to the periphery of the spleen in both  
10 control and SMA mice. This continues into the mid-symptomatic stage (P5, **E**)  
11 however there is a significant increase in cell death in the periphery of the SMA  
12 spleen (\*\* $p < 0.0001$ ), particularly around the splenic capsule. By the late-  
13 symptomatic stage (P8, **F**) there is no difference in occurrence of cell death between  
14 the control and SMA spleens. Scale bar = 50 $\mu$ m.  
15

1 Figure 3. **A morphologically distinct white pulps fails to develop and the spleen**  
2 **begins to degenerate in SMA mice**  
3 H&E staining of late-symptomatic (p8) spleens. **A.** In the control spleen, white pulp  
4 (dotted line) is clearly separated from red pulp. **D.** In the SMA spleen red and white  
5 pulp are indiscernible from one another, and there is an accumulation of large cells  
6 with lobulated nuclei (arrowhead, **G**). Scale bar: 50µm. **B.** Control spleen displays an  
7 intact splenic capsule, whereas the SMA spleen lacks a smooth and organised  
8 capsule-like structure, instead presenting apparent dissociation of capsular cells (**E**).  
9 Scale bar = 20µm. **C, F.** Picro-Sirius Red staining of the collagen component of the  
10 splenic capsule and trabeculae (arrowhead) in the control and late-symptomatic (p8)  
11 spleen. The splenic capsule and trabeculae are intact in the control spleen (**C**),  
12 however the SMA spleen lacks trabeculae, and shows dissociation of the capsule (**F**).  
13 Scale bar = 50µm.  
14



- 1 **Figure 4. The intrinsic vasculature of the spleen is unaltered in SMA**
- 2 Endothelial cell marker PECAM-1 stained vasculature throughout spleens of pre-,
- 3 mid- and late-symptomatic mice. Distribution of vasculature appears uniform
- 4 throughout the tissue of both control and SMA tissue. Analysis of fractional vessel
- 5 area indicates no change during development and no significant differences between
- 6 control and SMA at any time point. Scale bar = 50 $\mu$ m.
- 7

For Peer Review Only

1 Figure 5. **B cells fail to accumulate in SMA spleen and circulating lymphocyte count is**  
2 **reduced**  
3 B cell marker CD45R (green) demonstrates clusters of B cells have begun forming follicles  
4 in mid (P5)- and late (P8)-symptomatic control spleens, but not in mid- to late-  
5 symptomatic SMA spleens where B cells are absent. Circulating lymphocyte counts were  
6 significantly decreased in SMA mice (SMA n=4, control n=4; \*\* p<0.005). Scale bar =  
7 100µm.  
8

For Peer Review Only

1 Figure 6. **Megakaryocytes persist in SMA spleen but platelet numbers are unaltered**  
2 CD41 stained cells in p8 spleens from control (A) and SMA (B) mice. There are  
3 significantly greater numbers of positively stained CD41<sup>+</sup> nucleated megakaryocytes  
4 (inset) PUA present in the late-symptomatic (P8) SMA spleen compared with the  
5 control spleen (C). (\*\*\*\*p<0.0001). Scale bar = 25µm.

6  
7

For Peer Review Only

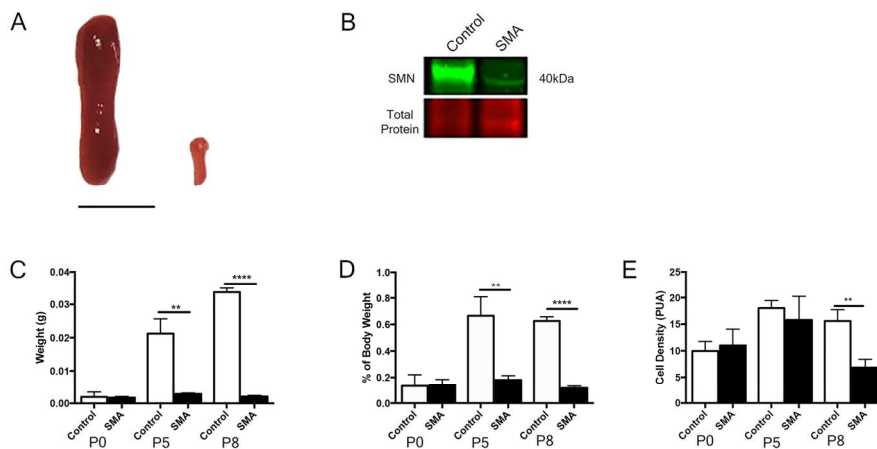


Figure 1. SMA spleen is disproportionately small and disorganised  
 A. Spleen from control (left) and late symptomatic (P8) SMA (right) mice. SMA spleen appears dramatically smaller and pale in comparison to control spleen. Scale bar = 5mm. B. Quantitative western blot of SMN protein (green) displays a significant reduction of SMN (~40kDa) in late-symptomatic (P8) SMA spleens ( $p < 0.0001$ ; ~39%) compared with controls. C. Spleen weights at pre- (P0), mid- (P5), and late-symptomatic (P8) time points. SMA spleens are significantly smaller than control spleens at both P5 (\*\* $p < 0.005$ ) and P8 (\*\*\*\* $p < 0.0001$ ). D. As a percentage of total body weight, spleens are significantly smaller at both p5 (\*\*  $p < 0.05$ ) and P8 (\*\*\*\* $p < 0.0001$ ). E. Quantification shows a significantly reduced density of cells in the SMA spleen (\*\* $p < 0.01$ ).

148x73mm (300 x 300 DPI)

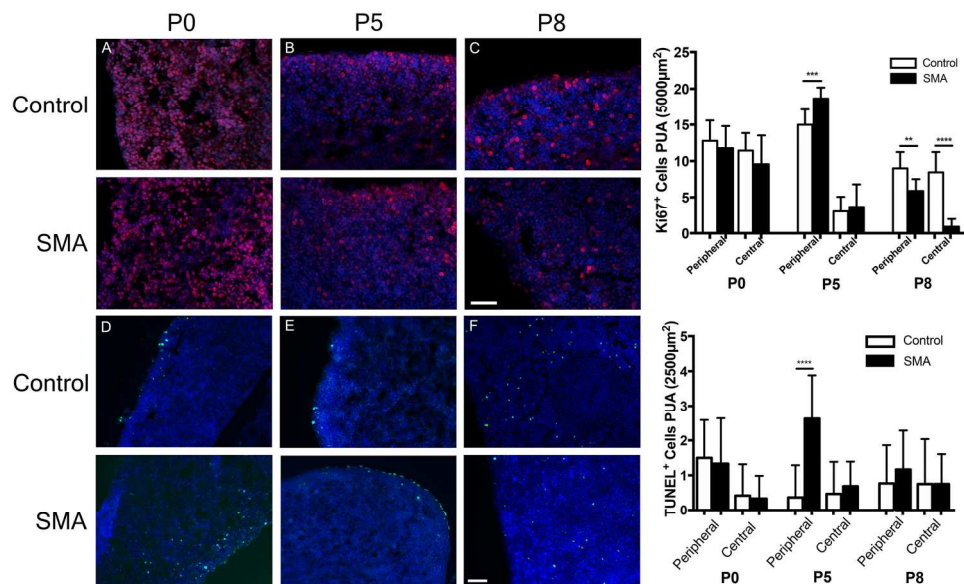


Figure 2. Cell proliferation and cell death are altered in the SMA spleen. Cell proliferation marker Ki67 (red) and cell death marker TUNEL (green) staining of pre-, mid- and late-symptomatic mice. A. At the pre-symptomatic stage (P0) cell proliferation is occurring uniformly throughout splenic tissue in both control and SMA mice. B. At the mid-symptomatic stage (P5) there is a significant increase in cell proliferation in the periphery of the SMA spleen ( $***p<0.005$ ). C. At the late-symptomatic stage (P8) cell proliferation is significantly reduced both centrally ( $****p<0.0001$ ) and peripherally ( $**p<0.01$ ) in SMA mice. Scale bar = 100µm. D. At birth (P0), apoptosis is largely restricted to the periphery of the spleen in both control and SMA mice. This continues into the mid-symptomatic stage (P5, E) however there is a significant increase in cell death in the periphery of the SMA spleen ( $****p<0.0001$ ), particularly around the splenic capsule. By the late-symptomatic stage (P8, F) there is no difference in occurrence of cell death between the control and SMA spleens. Scale bar = 50µm.

182x111mm (300 x 300 DPI)

Only

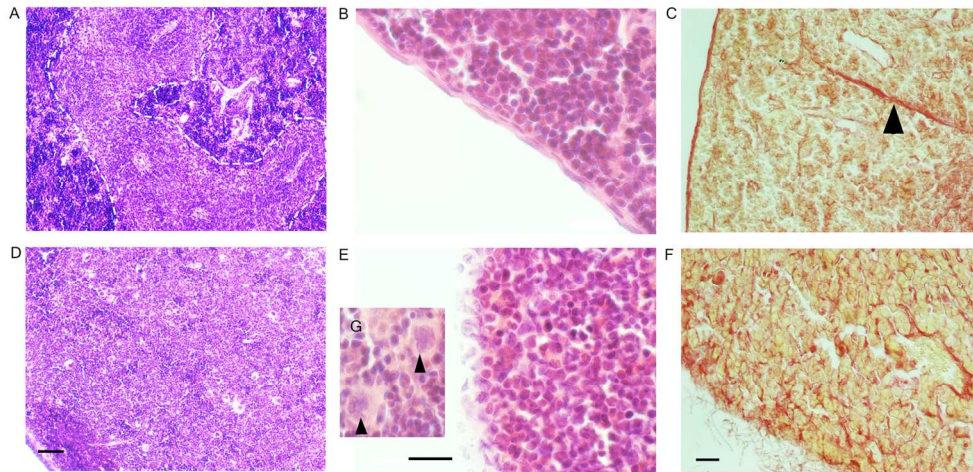


Figure 3. A morphologically distinct white pulps fails to develop and the spleen begins to degenerate in SMA mice

H&E staining of late-symptomatic (p8) spleens. A. In the control spleen, white pulp (dotted line) is clearly separated from red pulp. D. In the SMA spleen red and white pulp are indiscernible from one another, and there is an accumulation of large cells with lobulated nuclei (arrowhead, G). Scale bar: 50µm. B. Control spleen displays an intact splenic capsule, whereas the SMA spleen lacks a smooth and organised capsule-like structure, instead presenting apparent dissociation of capsular cells (E). Scale bar = 20µm. C, F. Picro-Sirius Red staining of the collagen component of the splenic capsule and trabeculae (arrowhead) in the control and late-symptomatic (p8) spleen. The splenic capsule and trabeculae are intact in the control spleen (C), however the SMA spleen lacks trabeculae, and shows dissociation of the capsule (F). Scale bar = 50µm.

151x76mm (300 x 300 DPI)

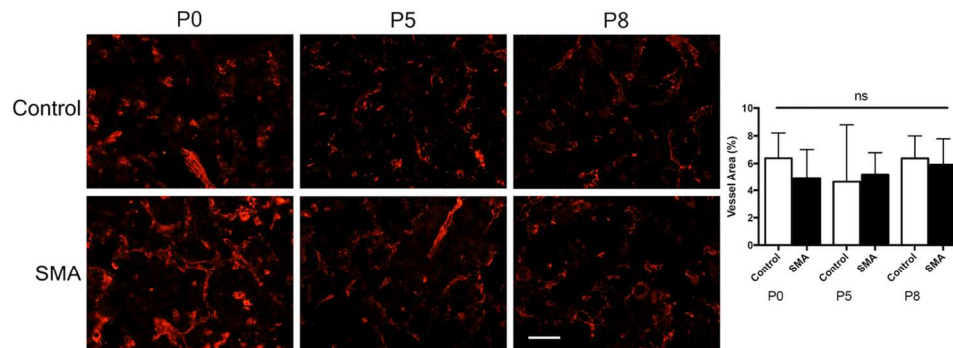


Figure 4. The intrinsic vasculature of the spleen is unaltered in SMA. Endothelial cell marker PECAM-1 stained vasculature throughout spleens of pre-, mid- and late-symptomatic mice. Distribution of vasculature appears uniform throughout the tissue of both control and SMA tissue. Analysis of fractional vessel area indicates no change during development and no significant differences between control and SMA at any time point. Scale bar = 50 $\mu$ m.

110x40mm (300 x 300 DPI)

Review Only

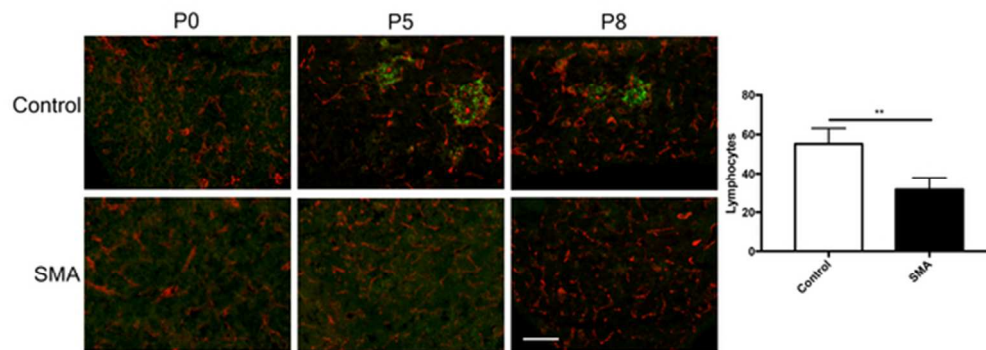


Figure 5. B cells fail to accumulate in SMA spleen and circulating lymphocyte count is reduced. B cell marker CD45R (green) demonstrates clusters of B cells have begun forming follicles in mid (P5)- and late (P8)-symptomatic control spleens, but not in mid- to late-symptomatic SMA spleens where B cells are absent. Circulating lymphocyte counts were significantly decreased in SMA mice (SMA n=4, control n=4; \*\* p<0.005). Scale bar = 100µm.

54x20mm (300 x 300 DPI)

Review Only



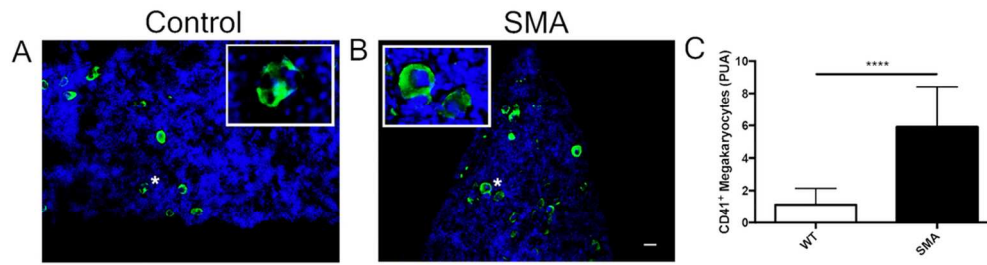


Figure 6. Megakaryocytes persist in SMA spleen but platelet numbers are unaltered CD41 stained cells in p8 spleens from control (A) and SMA (B) mice. There are significantly greater numbers of positively stained CD41+ nucleated megakaryocytes (inset) PUA present in the late-symptomatic (P8) SMA spleen compared with the control spleen (C). (\*\*\*\* $p < 0.0001$ ). Scale bar = 25 $\mu$ m.

95x30mm (300 x 300 DPI)

er Review Only

Table 1.

<b>Age (months)</b>	<b>Abnormalities</b>
6	Accessory spleen
14	Congested red pulp
16	Accessory spleen
21	None
28	Increased white pulp and erythroid precursors
33	None
35	None
45	Congested red pulp
60	None

SMA Type I routine spleen autopsy results